Journal of Functional Foods 108 (2023) 105713

Contents lists available at ScienceDirect

Journal of Functional Foods

journal homepage: www.elsevier.com/locate/jff

Effects of high dietary chicken protein on obesity development of rats fed high-fat diets

Shangxin Song [a,b,*], Yulin Gao [a], Tianlan Xia [a], Yefei Zhou [a], Guido J.E.J. Hooiveld [c], Michael Muller [d], Chunbao Li [b,*]

[a] School of Food Science, Nanjing Xiaozhuang University, 3601 Hongjing Road, Nanjing 211171, People's Republic of China
[b] Key Laboratory of Meat Processing and Quality Control, MOE Key Laboratory of Animal Products Processing, MOA Jiangsu Synergetic Innovation Center of Meat Processing and Quality Control, Nanjing Agricultural University, Nanjing 210095, People's Republic of China
[c] Nutrition, Metabolism and Genomics Group, Division of Human Nutrition, Wageningen University, Wageningen 6700 HB, the Netherlands
[d] Norwich Medical School, University of East Anglia, Norwich NR4 2QR, England

ARTICLE INFO

Keywords:
Blood insulin
Body fat accumulation
High meat protein diet
Lipid metabolism
Transcriptomics

ABSTRACT

This study explored the effects of dietary chicken protein at high (HCK, 40 % E) or normal (CK, 20 % E) levels on obesity development of rats fed high-fat diets. Compared with the CK diet, the HCK diet reduced body weight gain (by 15 %), epididymal adipose tissue mass (by 18.4 %), and adipocyte size (by 18.8 %) significantly without affecting the food intake of rats. It also reduced blood insulin and glycosylated serum protein (GSP) significantly by 45.4 % and 14.3 %, respectively; however, the OGTT and HOMA-IR results were not different. The HCK diet downregulated EAT transcriptomics related to the biosynthesis of cholesterol, triglycerides, and fatty acids, which were highly correlated with the most downregulated hub genes, *Insig1*, *Srebf2*, *Hmgcs1*, and *Fasn*. Therefore, high dietary chicken protein content reduced body fat accumulation, blood insulin, and GSP, and downregulated EAT transcriptomics related to lipid biosynthesis in rats fed high-fat diets.

1. Introduction

Obesity is a major global public health concern. Protein-rich diets have been popular for weight loss since the late 1950 s, and remain popular today (Iannitti & Palmieri, 2010). Currently, millions of people worldwide follow popular high-protein diets in the form of the Atkins diet, South Beach diet, etc. (Pesta & Samuel, 2014). Several experimental studies have confirmed that high-protein (and low-carbohydrate) diets are effective in preventing high-fat diet induced obesity (Magkos, 2020). However, most of these studies were primarily based on dairy proteins, such as casein and whey (Magkos, 2020). Little is known about how meat proteins modulate obesity response to high protein intake.

Meat is a nutritious animal-derived dietary protein (Salter, 2018). The global demand for meat continues to rise, and poultry (especially chicken) accounts for an increasingly large share of consumption (Heinrich Böll Stiftung, Friends of the Earth Europe & Bund für Umwelt und Naturschutz, 2021). Recently, several epidemiological studies have linked excessive meat consumption to obesity and type 2 diabetes (Salter, 2018). Some experimental studies in mice have reported that high-protein diets based on meat (chicken or pork) are more obesogenic than those based on casein (Liisberg et al., 2016). However, our previous

Abbreviations: AUC, area under curve; BWG, the body weight gain of rats from day 0 to day 84; BATW, brown adipose tissue weight; CK, high fat 20 % E chicken protein group; DBWG, the daily body weight gain of rat during 84-day feeding; DEI, the daily energy intake of rats during 84-day feeding; DFI, the daily feed intake of rats; DRGs, differentially expressed downregulated genes; EAT, epididymal adipose tissue; EATW, epididymal adipose tissue weight; EATW/FBW, relative percent content of epididymal adipose tissue to the final body weight of rats; FBW, the final body weight of rats on day 84; FC, fold change; FDR, false discovery rate; GO, Gene Ontology; GSEA, gene set enrichment analysis; GSP, glycosylated serum protein; HCK, high fat 40 % E chicken protein group; HOMA-IR, homeostasis model assessment for insulin resistance; IL, interleukin; KEGG, Kyoto Encyclopedia of Genes and Genomes; MCP-1, monocyte chemoattractant protein-1; OGTT, oral glucose tolerant test; PATW, perirenal adipose tissue weight; PCC, *Pearson* correlation coefficients; SREBP, sterol regulatory element binding protein; TNF-α, tumor necrosis factor α; WAT, white adipose tissue; WATW, white adipose tissue weight.

* Corresponding authors at: Weigang 1#, Nanjing 210095, PR China (Dr. Chunbao Li). Hongjing 3601#, Nanjing 211171, P.R. China (Dr. Shangxin Song).
E-mail addresses: ssxbxh2005@163.com (S. Song), 1918663805@qq.com (Y. Gao), 490942157@qq.com (T. Xia), yefeizhou@njxzc.edu.cn (Y. Zhou), guido.hooiveld@wur.nl (G. J.E.J. Hooiveld), Michael.Muller@uea.ac.uk (M. Muller), chunbao.li@njau.edu.cn (C. Li).

https://doi.org/10.1016/j.jff.2023.105713
Received 15 May 2023; Received in revised form 23 July 2023; Accepted 29 July 2023
Available online 5 August 2023

study showed that the intake of high levels of casein, chicken, and pork proteins was equally effective at reducing body fat mass in rats fed a high-fat diet (Song et al., 2020). Therefore, the effects of a high meat protein diet on body fat accumulation remain controversial.

Obesity is characterized by excessive body weight gain, abnormal adiposity, chronic low-grade systemic inflammation, insulin resistance, and related metabolic disorders, such as adipose tissue dysfunction (Heymsfield & Wadden, 2017). In order to clarify the effects of a high chicken protein diet on obesity development, this study fed rats high-fat diets with high (40 % E) or normal (20 % E) levels of chicken protein for 12 weeks. Changes in body weight, body fat mass, fasting blood insulin, glycosylated serum protein (GSP), adipokines, and inflammatory factors were monitored. A homeostasis model assessment for insulin resistance (HOMA-IR) was also calculated. The blood glucose clearance ability of rats was measured using an oral glucose tolerance test (OGTT). White adipose tissue (WAT) is the main organ for fat storage and plays an essential role in the regulation of lipid and energy homeostasis (Tchkonia et al., 2013). Therefore, the transcriptomics of the epididymal adipose tissue (EAT) was investigated to identify differentially expressed genes and related metabolic pathways. This research promotes an understanding of the physiological functions and health effects of dietary chicken proteins.

2. Materials & methods

2.1. Protein source and diets

Chicken protein source consisting of>90 % protein was prepared, as previously described (Song et al., 2020). Briefly, chicken breast fillets were cooked, freeze-dried, and defatted with methylene chloride/methanol (2:1, v:v). Chicken fat and protein may have different effects on the development of obesity; therefore, to clarify the role of chicken protein, defatted chicken meat was used. The amino acid composition of chicken protein (Supplementary Table 1) has been previously reported (Song et al., 2016). Low fat diet (LF group) was prepared according to formula of Research Diet D12450H (10 % E fat, 20 % E protein, 70 % E carbohydrates). High fat (from lard) diet with chicken protein (CK group) was prepared according to Research Diet D12451 (45 % E fat, 20 % E protein, 35 % E carbohydrate). Isocaloric high-fat-high-protein diet with chicken protein (HCK group) was prepared by increasing protein but reducing sucrose and removing starch and maltodextrin from D12451 (45 % E fat, 40 % E protein, 15 % E carbohydrate, D12451m). The formulas for D12450H, D12451, and D12451m are shown in Supplementary Table 1.

2.2. Animals and sample collection

All animals were handled in accordance with the guidelines of the Ethics Committee of the Experimental Animal Center of the China Pharmaceutical University (license number: SYXK (Su) 2018–0019). After a one-week adaption period, 21 male 6-week *Wistar* rats, with an initial body weight of 180–200 g, were randomly assigned to three groups (n = 7 rats in each group) and were fed LF, CK, and HCK diets, respectively, for 12 weeks. The rats were housed in a temperature-controlled room (23 ± 2 °C) on a 12:12 h light/dark cycle and had access to water and food, *ad libitum*. Food intake and body weight were measured at 9 am every three days. On day 84, the rats were deprived of food but given free access to water for 6 h before sacrifice. Blood was collected, and serum was isolated. Epididymal and perirenal white fat pads and brown fat pads between the scapulae of rats were obtained and weighed. All samples were snap frozen in liquid nitrogen and stored at −80 °C until analysis.

2.3. Histology of epididymal adipose tissue

Sections of epididymal adipose depots were fixed in 4 % formaldehyde in 0.1 M phosphate buffer, dehydrated, embedded, and stained with hematoxylin and eosin. Images of the adipose sections were acquired using an OLYMPUS BX53 light microscope (Olympus Imaging Corporation, Tokyo, Japan) equipped with an SC180 camera at 200 × magnification. Histomorphometry was performed to evaluate the adipocyte area and number using Image-Pro Plus software (version 6.0; Media Cybernetics, Inc., Rockville, MD, USA). One field per sample and seven samples from each group were analyzed. The area was calculated from the average value of the top six large cell areas in one field. The total number of cells in each field was counted manually. For incomplete cells at the edge of the visual field, only the upper and lower cells were counted.

2.4. Oral glucose tolerant test (OGTT)

The OGTT was conducted on day 80 at 1 pm, as previously described (Song et al., 2020). Briefly, 6-h fasting rats were administered 2 g glucose/kg body weight by gavage, and tail vein blood drops were collected for glycemia measurement before (0 min) and after glucose gavage (30, 60, 90, and 120 min) using a glucometer (Jiangsu Yuyue Medical Equipment & Supply Co. Ltd., Shanghai, China). The area under the curve (AUC) was calculated.

2.5. Blood parameters detections

Serum was collected on day 84 from fasted rats. Insulin, adiponectin, and resistin concentrations were detected using ELISA kits (E-EL-R2466c, E-EL-R0329c, and E-EL-R0614c, Elabscience Biotechnology Co., Ltd., Wuhan, Hubei, China) according to the manufacturer's instructions. Serum leptin concentrations were detected using Bio-Plex Pro Rat Diabetes Leptin kits (171L7006, Bio-Rad Laboratories, Inc., Hercules, CA, USA) according to the manufacturer's instructions. Serum concentrations of inflammatory factors, including tumor necrosis factor-α (TNF-α), monocyte chemoattractant protein-1 (MCP-1), interleukin (IL)-6, IL-1b, and IL-10 were detected using Bio-Plex Cytokine Express 5-Plex (17001657, Bio-Rad Laboratories, Inc.) according to the manufacturer's instructions. Serum glucose and GSP levels were measured using an automatic biochemical analyzer (Rayto Life and Analytical Sciences Co., Ltd., Shenzhen, China). The HOMA-IR was calculated according to the equation HOMA-IR = (fasting insulin in mU/L × fasting glucose in mM)/22.5 (Cacho, Sevillano, Castro, Herrera, & Ramos, 2008).

2.6. Gene expression profiling in adipose tissue using RNA-sequencing

2.6.1. RNA extraction

Total RNA was extracted from the EAT of three rats from each group using the TRIzol Reagent according to the manufacturer's instructions (Invitrogen, CA, USA), and genomic DNA was removed using DNase I (TaKara, Dalian, China). RNA quality was determined using a 2100 Bioanalyzer (Agilent, Beijing, China) and quantified using ND-2000 (NanoDrop Technologies). Only high-quality RNA samples ($OD_{260/280}$ = 1.8–2.2, $OD_{260/230} \geq 2.0$, RIN ≥ 6.5, 28S:18S ≥ 1.0, >1 μg) were used to construct the sequencing library.

2.6.2. Library Preparation, and Illumina HiSeq xten/Nova seq 6000 sequencing

RNA-seq was performed by Major Bio (Shanghai, China). The RNA-seq transcriptome library was prepared using the TruSeqTM RNA sample preparation Kit from Illumina (San Diego, CA, USA) using 1 μg of total RNA. Briefly, mRNA was isolated according to the poly (A) selection method using oligo (dT) beads and then fragmented using fragmentation buffer. Double-stranded cDNA was synthesized using a SuperScript double-stranded cDNA synthesis kit (Invitrogen, Carlsbad, CA, USA) with random hexamer primers (Illumina). Then the synthesized cDNA was subjected to end-repair, phosphorylation and 'A' base

addition according to Illumina's library construction protocol. Libraries were size-selected for cDNA target fragments of 300 bp on 2 % Low Range Ultra Agarose, followed by PCR amplification using Phusion DNA polymerase (New England Biolabs, Ipswich, MA, USA) for 15 PCR cycles. After quantification using TBS380, the paired-end RNA-seq library was sequenced using an Illumina HiSeq Xten/NovaSeq 6000 sequencer (2 × 150 bp read length).

2.6.3. Read mapping

Raw paired-end reads were trimmed and quality controlled using SeqPrep (https://github.com/jstjohn/SeqPrep) and Sickle (https://github.com/najoshi/sickle) with default parameters. Clean reads were separately aligned to *Rattus norvegicus* genome (Rnor_6.0, https://www.ensembl.org/Rattus_norvegicus/Info/Index) with orientation mode using HISAT2 software (https://ccb.jhu.edu/software/hisat2/index.shtml). The mapped reads of each sample were assembled using StringTie (https://ccb.jhu.edu/software/stringtie/index.shtml?t = example) with a reference-based approach.

2.6.4. Identification of differentially expressed genes

Nonspecific filtering of the count table was carried out to increase the detection power (Bourgon, Gentleman, & Huber, 2010), based on the requirement that a gene should have an expression level greater than one count per million reads, mapped for at least three libraries across all samples. We adjusted for differences in library size using the trimmed mean of M−values normalization method (Robinson & Oshlack, 2010), implemented in the Bioconductor package edgeR (Robinson, McCarthy, & Smyth, 2010). Counts were then log-transformed and the observed mean–variance trend was converted into precision weights using the voom function (Law, Chen, Shi, & Smyth, 2014) in the Bioconductor package *limma* (Ritchie et al., 2015). Differentially expressed genes were identified using linear models and moderated t-statistics (Ritchie et al., 2015). The Benjamini-Hochberg False Discovery Rate method was used to correct raw *P* value. Genes that satisfied the criterion of $P < 0.05$ were considered to be significantly regulated.

2.6.5. Biological interpretation of gene expression Data

Gene expression changes are related to biologically meaningful changes using gene set enrichment analysis (GSEA) (Subramanian et al., 2005). Gene sets were retrieved from Gene Ontology (GO), National Cancer Institute, Kyoto Encyclopedia of Genes and Genomes (KEGG), Biocarta, Pfam, Reactome, and Wiki Pathway databases. Only gene sets consisting of>15 genes and<500 genes were considered, resulting in the inclusion of 3386 gene sets. For each comparison, the genes were ranked by their t-values, which were calculated using the empirical Bayes method. The statistical significance of the GSEA results was determined using 1000 permutations. The Enrichment Map v3.3.3 plugin for Cytoscape v3.8.2 was used to visualize and interpret the GSEA results (Merico, Isserlin, Stueker, Emili, & Bader, 2010). Enrichment maps were generated using gene sets that passed conservative significance thresholds (False Discovery Rate (FDR) < 0.05). The interactions and functional enrichment of differentially expressed genes were retrieved from the STRING v11.5 database using default parameters, and the networks were visualized using Cytoscape v3.8.2.

2.6.6. Quantitative PCR (Q-PCR) verifying downregulated genes

The top six downregulated genes related to lipid metabolism, including *Insig1* (insulin induced gene 1), *Ptgis* (prostaglandin I2 synthase), *Angptl4* (angiopoietin-like 4), *Hmgcs1* (3-hydroxy-3-methylglutaryl-CoA synthase 1), *Fasn* (fatty acid synthase), and *Srebf2* (sterol regulatory element binding transcription factor 2) were verified using Q-PCR. *Gapdh* (glyceraldehyde-3-phosphate dehydrogenase) was used as a housekeeping gene. Primers used are listed in Supplementary Table 2. The iScript cDNA Synthesis Kit (Bio-Rad Laboratories, Inc.) was used to synthesize cDNA. Q-PCR was performed using an iTaq Univer SYBR Green Supermix (Bio-Rad Laboratories, Inc.) on a CFX96 Real-Time System (Bio-Rad Laboratories, Inc.). Gene expression changes of the HCK vs. CK group were calculated using the $2^{-\Delta\Delta CT}$ method.

2.7. Statistical analysis

Except for the RNA-seq data, all statistical analyses were performed using SPSS (version 20.0; SPSS Inc., Chicago, IL, USA). Comparisons between the LF and CK groups, and between the CK and HCK groups were performed. Therefore, an independent sample T test was performed for the two comparisons. Statistical significance was set at $P < 0.05$. Values are shown as means ± SE. Correlations between significant features were analyzed using the *Pearson* method.

3. Results

3.1. Body weight gain and food intake

Rats were fed LF and HF diets with CK or HCK levels of chicken protein, respectively, for 12 weeks. The LF and CK groups were compared to test whether the obesity model could be successfully established after 12 weeks of treatment. Comparisons between the CK and HCK groups were performed to test the effects of high dietary chicken protein on body fat regulation. The initial body weights of the rats did not differ significantly (Fig. 1A). During the 12-week treatment period, body weight change plateaued between weeks 2 and 6 (Fig. 1A). From the tenth week, the body weights of the rats fed the CK diet were significantly higher than those of the rats fed the LF diet ($P < 0.05$). Moreover, rats in the CK group showed significantly higher body weight gain (BWG, Fig. 1C) and daily body weight gain (DBWG, Fig. 1D) than those in the LF group ($P < 0.05$), confirming that the obesity model was successfully established. Concurrently, the body weights of rats fed the HCK diet were lower than those of rats fed the CK diet from the ninth week ($P < 0.05$; Fig. 1A). At week 12, rats in the HCK group had 7.3 % lower body weight than rats in the CK group ($P < 0.05$, Fig. 1A), which could be attributed to 14.8 % reduced BWGs (Fig. 1C) and 15.4 % reduced DBWGs (Fig. 1D) in the HCK group compared to the CK group ($P < 0.05$).

Regarding the average daily food intake per week (Fig. 1B), the food intake of rats showed a downward trend (Fig. 1B) from weeks 2 to 5 (rats were 8–11 weeks old), which could account for the corresponding plateau of body weight changes between weeks 2 and 6. Regarding the average daily food intake throughout the 12 weeks (Fig. 1E), no difference was observed between the LF and CK groups and the CK and HCK groups. However, the daily energy intake (DEI, Fig. 1F) of the rats was significantly higher in the CK group than that in the LF group ($P < 0.05$). The ratio of daily food intake (DFI) to DBWG was significantly lower for the CK group than for the LF group (Fig. 1G, $P < 0.05$), indicating a higher food efficiency of the CK diet than that of the LF diet. However, the HCK diet had a significantly higher DFI/DBWG than the CK diet (27.9 %, $P < 0.05$), indicating a lower food efficiency of the HCK diet than CK diet.

3.2. Body fat mass and EAT morphology

Compared to the LF diet (Fig. 2), the CK diet significantly increased epididymal (EATW), perirenal (PATW), and white adipose tissue weights (WATW = EATW + PATW) and their relative ratios to body weight (EATW/FBW, PATW/FBW, WATW/FBW, $P < 0.05$), but had no significant effects on brown adipose tissue weight (BATW and BATW/FBW). Compared to the CK diet, the HCK diet significantly reduced the EATW (by 24.3 %), EATW/FBW (by 18.4 %), WATW (by 21.4 %), and BATW (by 17.6 %, $P < 0.05$) in rats, but had no significant effects on PATW, PATW/FBW, WATW/ FBW, and BATW/FBW ($P > 0.05$). Histological examination of EAT (Fig. 2E) showed that adipocytes were normal and intact. The adipocyte size in the HCK group was significantly smaller than that in the CK group (18.8 %, $P < 0.05$). The number of

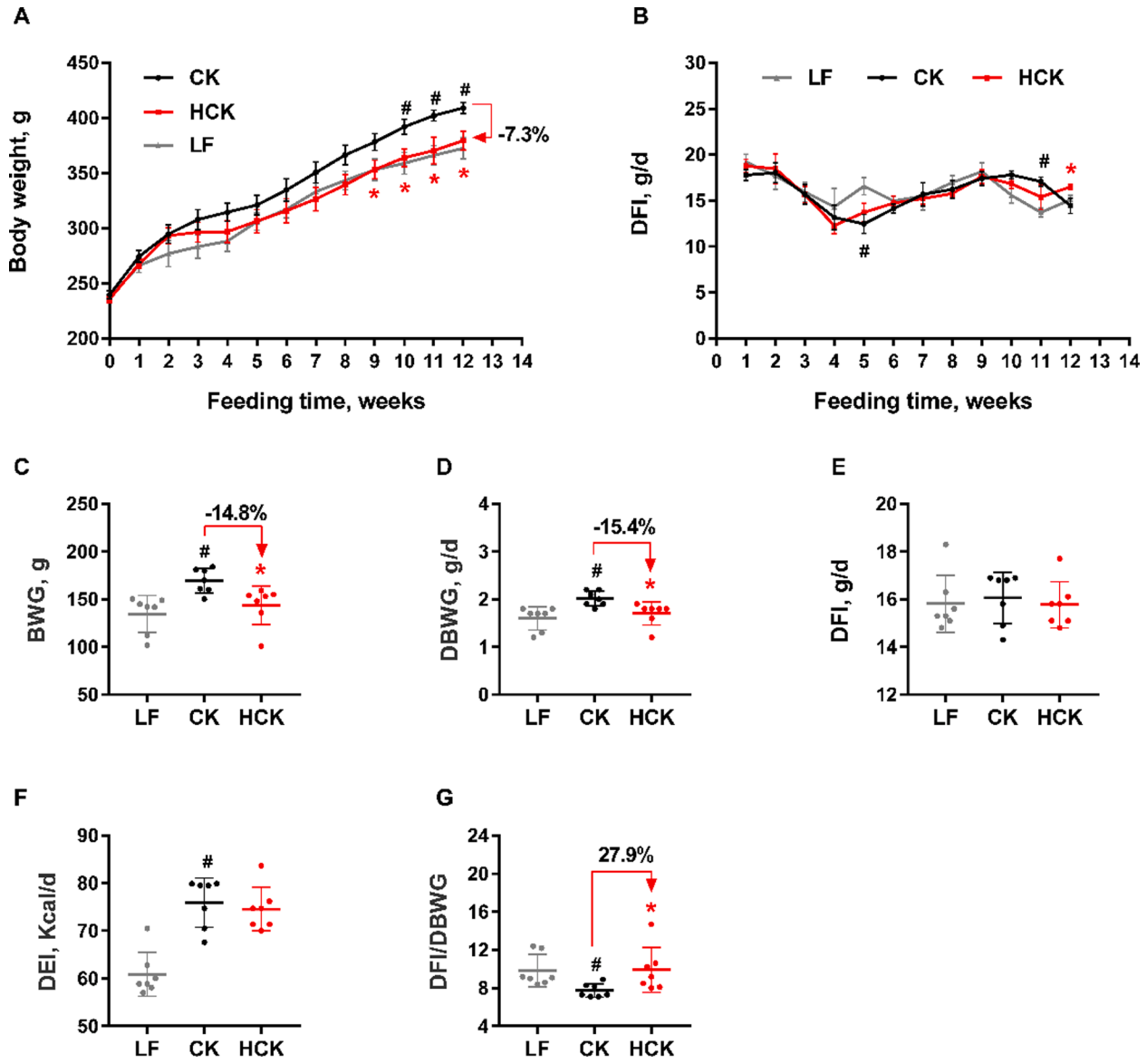

Fig. 1. Body weight gain and food intake of rats fed low-fat diet or high-fat diet with high or normal level of chicken protein. (A) weekly body weight of rats; (B) daily food intake (DFI) per week of rats; (C) the total body weight gain of rats from day 0 to day 84 (BWG); (D) the daily body weight gain of rat during 84-day feeding (DBWG); (E) the daily food intake of rats during 84-day feeding; (F) the daily energy intake of rats during 84-day feeding (DEI); (G) the ratio of DFI to DBWG. Note: LF: low-fat diet group; CK: high-fat 20% E chicken protein diet group; HCK: high-fat 40% E chicken protein diet group; DFI: daily food intake; BWG: body weight gain; DBWG: daily body weight gain; DEI: daily energy intake; Comparisons of the LF and CK groups and the CK and HCK groups were preplanned. Therefore, independent sample T test was carried out for the two comparisons. Values are shown as means ± SE; n = 7; # means significant difference ($P < 0.05$) between the LF and CK groups; * means significant difference ($P < 0.05$) between the CK and HCK groups; The numbers above the arrow indicate differences between CK and HCK groups calculated according to the equation (CK-HCK)/CK*100%.

adipocytes in the HCK group was higher than that in the CK group; however, the difference was not significant ($P > 0.05$).

3.3. OGTT and serum items

The OGTT was conducted on day 80 to measure the blood glucose clearance ability of rats (Fig. 3A & B). Compared with the CK group, the HCK group had significantly higher blood glucose levels 30 min after glucose gavage ($P = 0.05$). However, blood glucose levels at other time points, including 0, 60, 90, and 120 min after glucose gavage, and thus the value of the area under the curve (OGTT-AUC), were not different between the two groups. Moreover, HOMA-IR did not differ between the CK and HCK groups. However, serum GSP and insulin concentrations were reduced significantly by the HCK diet, by 14.3 % and 45.4 % ($P < 0.05$), respectively. Blood leptin and MCP-1 concentrations were also decreased by the HCK diet by 16.6 % and 38.0 %, respectively, but these differences were not significant (Fig. 4; $P > 0.05$). Changes in other serum adipokines (adiponectin and resistin) and inflammatory factors (TNF-α, IL-6, IL-1b, and IL-10) were not statistically significant (Fig. 4; $P > 0.05$).

3.4. Adipose tissue transcriptome

Considering the considerable changes in EAT mass, transcriptomic analysis of EAT was performed to reveal the mRNA transcription of adipocytes affected by increased dietary chicken protein. A totally of 10 493 nonredundant genes in the adipose tissue were annotated and quantified. Among these, 413 genes were downregulated and 350 genes were significantly upregulated ($P < 0.05$) by the HCK diet compared to the CK diet.

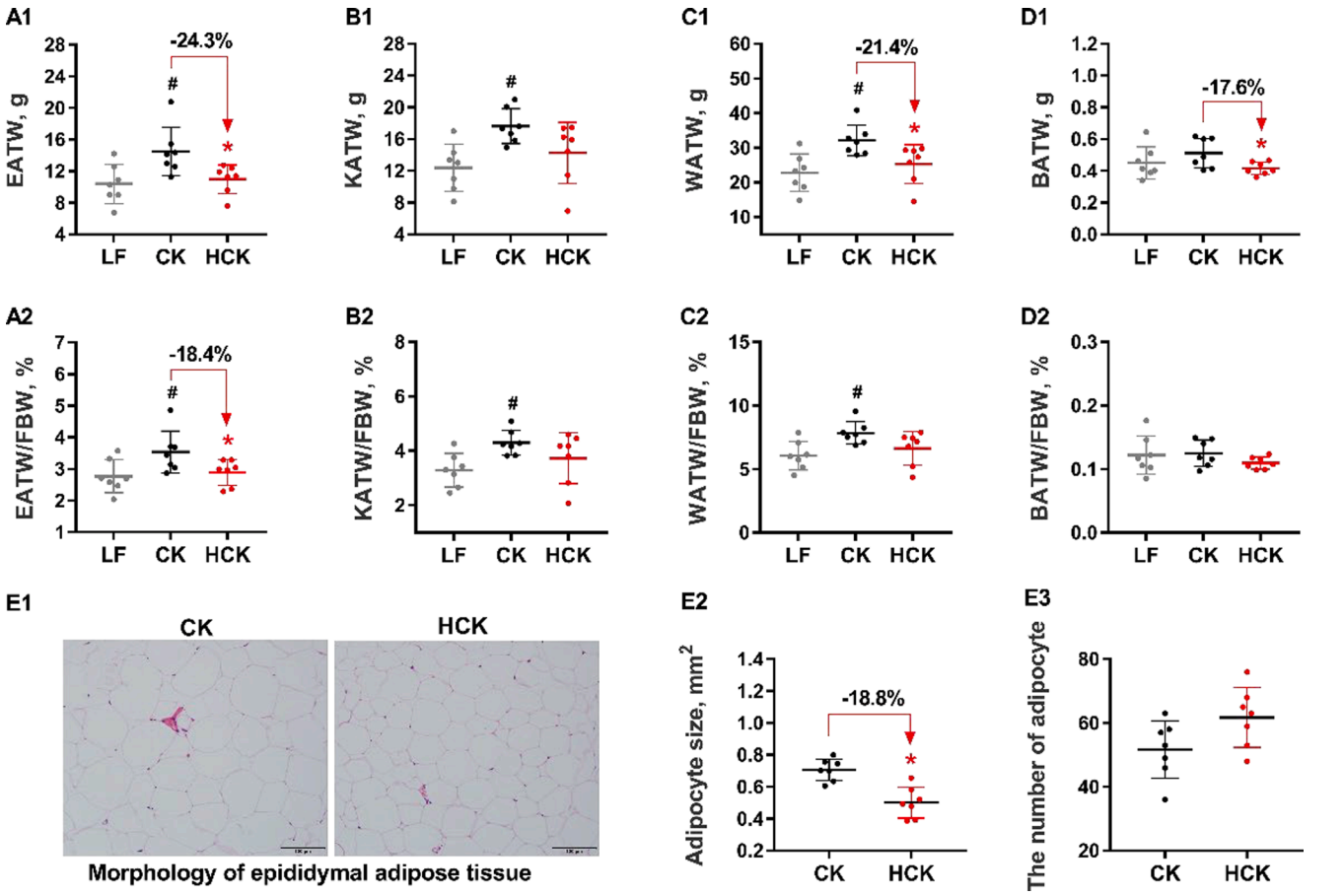

Fig. 2. Body fat mass and epididymal adipose tissue morphology of rats fed low-fat diet or high-fat diet with high or normal level of chicken protein. (A1) epididymal adipose tissue weight (EATW) of rats; (A2) relative percent content of epididymal adipose tissue to the final body weight (EATW/FBW) of rats; (B1) perirenal adipose tissue weight (PATW) of rats; (B2) relative percent content of perirenal adipose tissue to the final body weight (PATW/FBW) of rats; (C1) white adipose tissue weight (WATW = EATW + PATW) of rats; (C2) relative percent content of white adipose tissue to the final body weight (WATW/FBW) of rats; (D1) brown adipose tissue weight (BATW) of rats; (D2) relative percent content of brown adipose tissue to the final body weight (BATW/FBW) of rats; (E1) epididymal adipose tissue morphology; (E2) adipocyte area; (E3) the number of adipocyte. Note: LF: low-fat diet group; CK: high-fat 20% E chicken protein diet group; HCK: high-fat 40% E chicken protein diet group; Comparisons of the LF and CK groups and the CK and HCK groups were preplanned. Therefore, independent sample T test was carried out for the two comparisons. Values are shown as means ± SE; n = 7; # means significant difference ($P < 0.05$) between the LF and CK groups; * means significant difference ($P < 0.05$) between the CK and HCK groups; The numbers above the arrow indicate differences between CK and HCK groups calculated according to the equation (CK-HCK)/CK*100%.

GSEA of the quantified genes showed that 230 gene sets were significantly enriched (FDR-Q < 0.05, Fig. 5). Among these, only two gene sets of the TNF-receptor I and Fas pathways, which are related to apoptosis, were upregulated (FDR-Q < 0.05). The remaining 228 gene sets were significantly down-regulated (FDR-Q < 0.05). Among these, 60 gene sets were related to the cell cycle, and 38 gene sets were related to protein translation. Additionally, 67 downregulated gene sets were related to carbohydrate and energy metabolism, including glycolysis, gluconeogenesis, glucose catabolism, the TCA cycle, oxidative phosphorylation, and the electron transport chain. A total of 39 downregulated gene sets were related to lipid metabolism, including triglyceride, phospholipid, cholesterol, and fatty acid biosynthesis, and fatty acid beta oxidative catabolism.

To determine the relationships between the downregulated gene sets and differentially expressed downregulated genes (DRGs), the subsets of DRGs, including the Top 30, Top 50, Top 200–50, Top 300–200 and Top 413–300, overlapped with the GSEA map (Fig. 5). The "Top 50″ DRGs set mainly overlapped with the gene set clusters of lipid metabolism. The other DRGs subsets, including the Top 200–50, Top 300–200, and Top 413–300, mostly overlapped with the gene set clusters of energy metabolism, protein translation, and the cell cycle.

The interaction network (Fig. 6A) showed two large clusters of DRGs. One large cluster was enriched in the KEGG pathway of ribosomes and the GO biological process of gene expression (blue tone, Fig. 6C). Another large cluster was enriched in the KEGG pathway of oxidative phosphorylation and the GO biological process of carbohydrate derivative biosynthesis (yellowish-brown tone, Fig. 6C). However, the extent of DRGs downregulation in these two large clusters was relatively low (fold changes (FC) < 1.5, $P < 0.05$). At the same time, DRGs with a larger extent of change (FC > 2.0, $P < 0.05$) were mainly enriched in the GO biological processes of lipid, sterol, and fatty acid metabolism (green tone, Fig. 6C). The changes in the expression of interactive downregulated genes related to lipid metabolism are shown in Supplementary Table 3. To clearly demonstrate their interactions, a subnetwork of these genes was rebuilt (Fig. 6B). Several genes closely related to lipid metabolism were highly down regulated by the HCK diet (Table 1), including *Insig1*(FC = -3.2, $P = 0.031$), Srebf2 (FC = -1.46, $P = 0.030$), *Angptl4* (FC = -2.63, $P = 0.018$), *Hmgcs1* (FC = -1.46, $P = 0.030$), and *Fasn* (FC = -2.63, $P = 0.011$).

3.5. Q-PCR verifying downregulated genes

The six most downregulated genes related to lipid metabolism, including *Insig1*, *Ptgis*, *Angptl4*, *Hmgcs1*, *Fasn*, and *Srebf2*, were verified

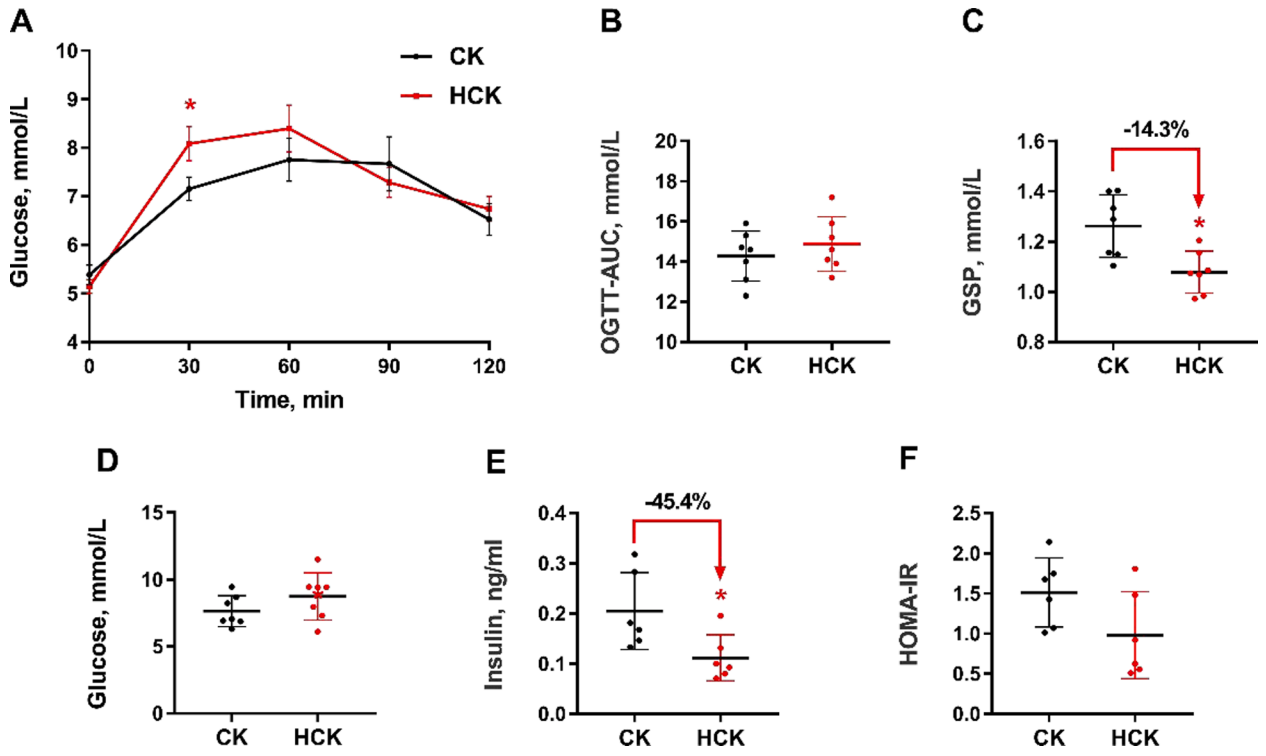

Fig. 3. Oral glucose tolerant test results, glycosylated serum protein and fasting serum glucose, insulin and HOMA-IR index of rats fed high-fat diet with high or normal level of chicken protein. (A) oral glucose tolerant test (OGTT) result on day 80; (B) area under curve of oral glucose tolerant test (OGTT-AUC); (C) glycosylated serum protein (GSP) on day 84; (D) fasting serum glucose on day 84; (E) fasting serum insulin on day 84; (F) The homeostasis model assessment for insulin resistance (HOMA-IR) calculated according to the equation HOMA-IR = (fasting insulin in mU/L × fasting glucose in mM)/22.5. Note: CK: high-fat 20% E chicken protein diet group; HCK: high-fat 40% E chicken protein diet group; Comparisons of the CK and HCK groups were carried out by using independent sample T test. Values are shown as means ± SE; n = 7; * means significant difference ($P < 0.05$); The numbers above the arrow indicate differences calculated according to the equation (CK-HCK)/CK*100%.

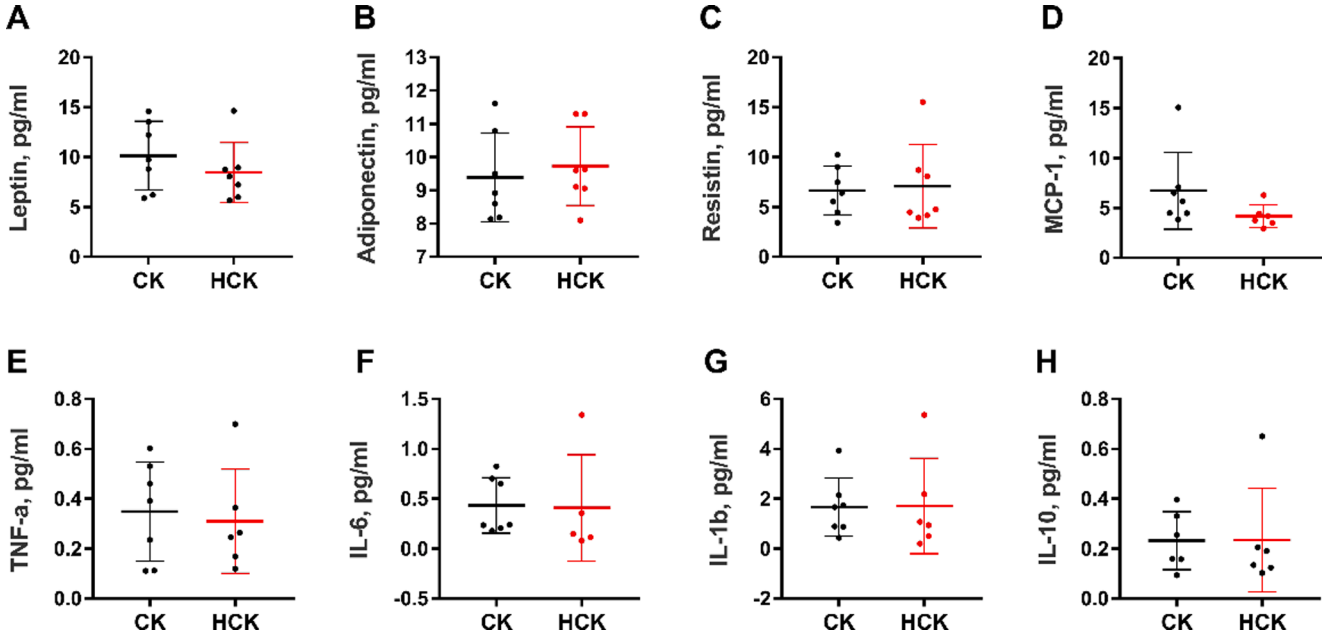

Fig. 4. Serum adipokines and inflammatory factors of rats fed high chicken protein compared to the rats fed normal chicken protein. (A) leptin; (B) adiponectin; (C) resistin; (D) MCP-1: monocyte chemoattractant protein-1; (E) TNF-α: tumor necrosis factor α; (F) IL-6: interleukin 6; (G) IL-1b: interleukin 1b; (H) IL-10: interleukin 10. Note: CK: high-fat 20% E chicken protein diet group; HCK: high-fat 40% E chicken protein diet group; Comparisons of the CK and HCK groups were carried out by using independent sample T test. Values are shown as means ± SE; n = 7; * means significant difference ($P < 0.05$); The numbers above the arrow indicate differences calculated according to the equation (CK-HCK)/CK*100%.

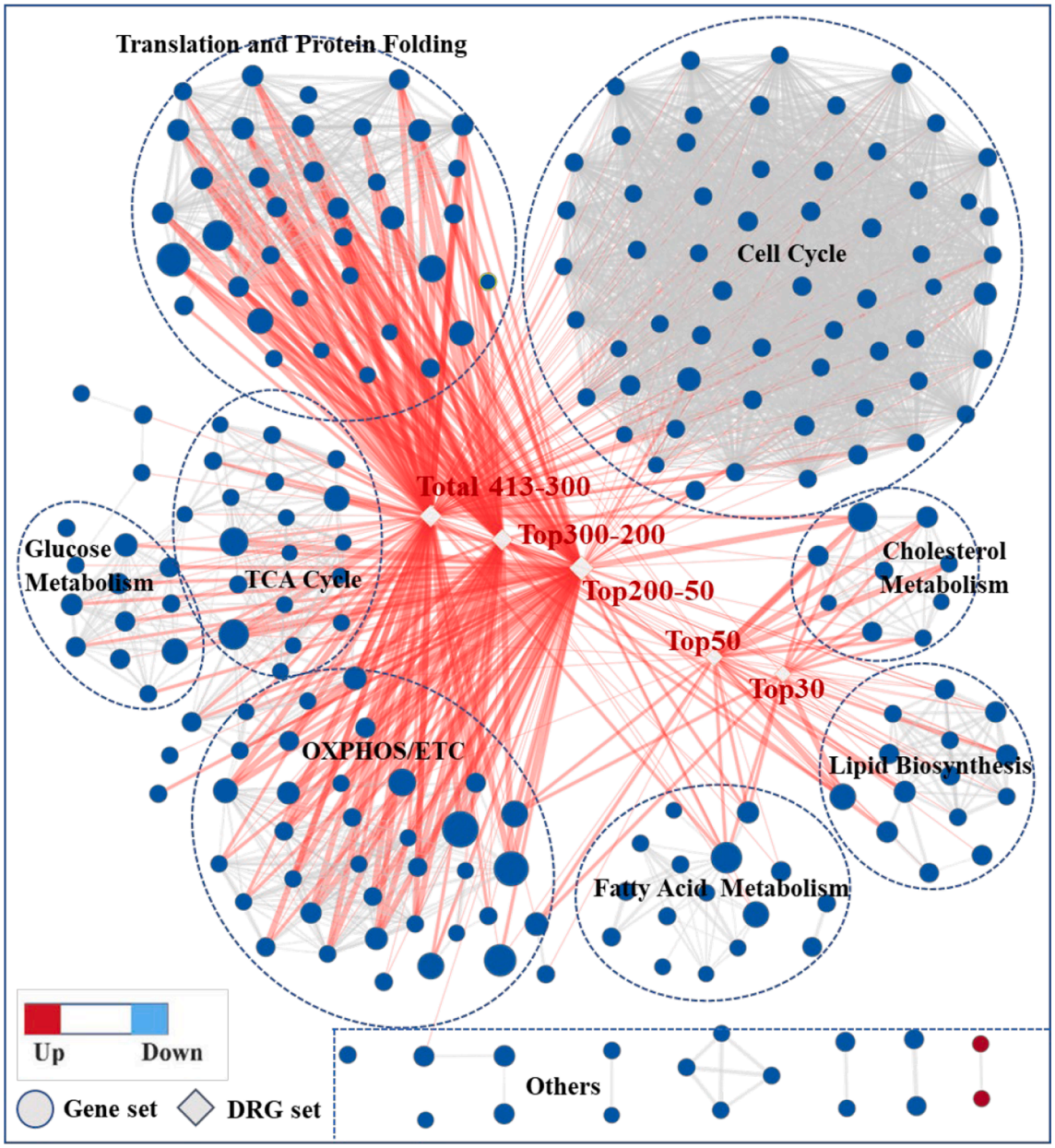

Fig. 5. Gene set network of epididymal adipose tissue transcriptome of rats fed high chicken protein compared to the rats fed normal chicken protein. Note: Enrichment map was generated with gene-sets that passed significance thresholds (False Discovery Rate (FDR)-Q < 0.05). The node size is proportional to the total number of genes within each gene-set (from 15 to 500). The red color of nodes indicate upregulation and blue for downregulation. The weighted grey lines between the round nodes represent the "overlap" score (Jaccard and overlap coefficients > 0.375) depending on the number of genes two gene-sets share. The more genes two gene-sets share, the wider the line. The grey diamonds in the map represent the set of downregulated genes (DRGs) and they were overlapped with putative target genes in the genes sets using the Post Analysis tool in the Enrichment Map plugin. When all DRGs are sorted according to their fold changes from large to small. The"Top 30" represents a set of the top 30 DRGs with the largest fold changes; The "Top 50" represent a set of the top 50 DRGs; The "Top 200–50" represent a set of the top 200 DRGs excluding the top 50 DRGs; The "Top 300–200" represent a set of the top 300 DRGs excluding the top 200 DRGs; The "Top 413–300" represent a set of the top 413 DRGs excluding the top 300 DRGs. Red lines represent the overlap P value < 0.05 (Fisher's Exact Test) between gene sets and downregulated genes. Nodes of high similarity were automatically arranged close together, and circles were semi-automatically annotated and manually labelled. "Others" on the figure represents nodes of low similarity, and thus were not arranged close together with other node clusters. The detailed information about nodes has been shown in the Supplementary Fig. 1. (For interpretation of the references to color in this figure legend, the reader is referred to the web version of this article.)

using QPCR. The FC of these genes showed good consistency between RNA-seq and Q-PCR detection (Table 1).

3.6. Correlations of significant features

The correlations between significant features are shown in Fig. 7. See *Pearson* correlation coefficients (PCC) and P-values in Supplementary Table 4. The adipocyte area positively correlated with the mRNA expression of *Insig1* and *Ptgis* (PCC > 0.84, $P < 0.05$). The mRNA expression of *Insig1* also positively correlated with the mRNA expression of *Fasn* and *Srebf2* (PCC > 0.85, $P < 0.05$) which positively correlated with the mRNA expression of *Hmgcs1* (PCC > 0.9, $P < 0.05$). Additionally, fasting blood insulin and GSP levels positively correlated with mRNA expression of *Angptl4* (PCC > 0.8, $P < 0.05$), which also positively correlated with *Ptgis* mRNA expression (PCC = 0.822, $P < 0.05$).

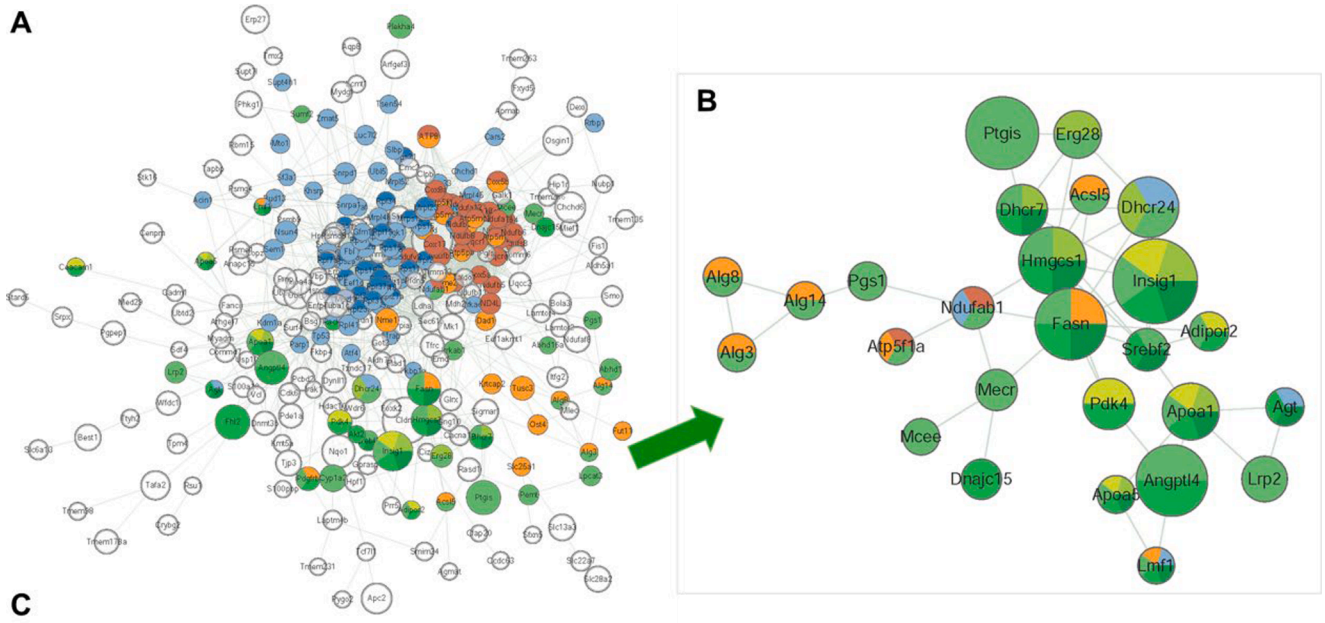

C

Category	Term name	Description	Chart color	Genes	P value	FDR value
GO Biological Process	GO:0006629	Lipid metabolic process		39/1190	5.30E-04	0.0387
GO Biological Process	GO:0019216	Regulation of lipid metabolic process		19/424	5.30E-04	0.0387
GO Biological Process	GO:0019218	Regulation of steroid metabolic process		9/121	6.40E-04	0.0442
GO Biological Process	GO:0016126	Sterol biosynthetic process		7/50	7.59E-05	0.0064
GO Biological Process	GO:0042304	Regulation of fatty acid biosynthetic process		6/47	3.90E-04	0.0292
KEGG Pathways	KEGG:00190	Oxidative phosphorylation		36/130	1.86E-28	6.26E-26
GO Biological Process	GO:1901137	Carbohydrate derivative biosynthetic process		30/602	1.90E-06	1.70E-04
GO Biological Process	GO:0010467	Gene expression		85/2056	2.43E-12	5.39E-10
KEGG Pathways	KEGG:03010	Ribosome		33/130	3.87E-25	4.34E-23

Fig. 6. Interactive network of downregulated genes and their enriched biological processes. (A) Interactive network of downregulated genes (DRGs); (B) the subnetwork of the DRGs enriched in GO biological process of lipid, sterol and fatty acid metabolism; (C) color legend of the enriched biological processes. Note: Nodes represent downregulated genes; The node size is proportional to the fold changes of genes; Node color represents enriched biological processes illustrated in the Fig. 5 C; Edges represent gene-gene associations.

Table 1
Expression changes of top downregulated genes related to lipid metabolism.

Gene ID	Symbol	Gene name	Fold changes	
			RNA-seq	qPCR
64,194	Insig1	insulin induced gene 1	−3.16*	−1.48*
25,527	Ptgis	prostaglandin I2 synthase	−2.68*	−2.25*
362,850	Angptl4	angiopoietin-like 4	−2.63*	−3.37*
50,671	Fasn	fatty acid synthase	−2.63*	−2.05*
29,637	Hmgcs1	3-hydroxy-3-methylglutaryl-CoA synthase 1	−2.47*	−2.27*
300,095	Srebf2	sterol regulatory element binding transcription factor 2	−1.46*	−1.86*

Note: FC: fold change of HCK group v. s. CK group.

4. Discussion

High-protein diets have become increasingly popular for the prevention of obesity (Carlin et al., 2019). However, the anti-obesity effects of a high meat protein diet remain controversial. This study aimed to clarify the effects of high dietary chicken protein on the development of obesity in rats fed a high-fat diet. Obesity develops as a result of chronic positive energy balance, i. e., energy intake exceeds energy expenditure (Drummen, Tischmann, Gatta-Cherifi, Adam, & Westerterp-Plantenga, 2018). In this study, the rats fed a high-fat diet with normal levels of chicken protein (CK group) gained more energy and, thus, more body weight and body fat mass than rats fed a low-fat diet (LF group),

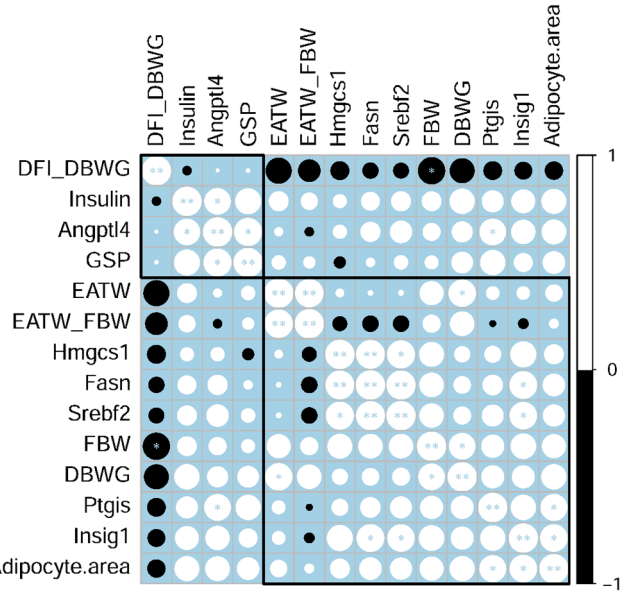

Fig. 7. Correlations of significant features. Note: Correlations of significant features were analyzed using Pearson method. * means significant at $P < 0.05$. ** means significant.

confirming that the obesity model was established successfully after 12 weeks of treatment. Food intake of rats varied over time. The increased food intake was due to the increased body weight of rats over time. The decreased food intake in the beginning might be due to the diet exchange. Notably, rats fed high-fat diet with high chicken protein (the HCK group) had similar food and energy intake to rats fed high-fat diet with normal chicken protein (the CK group) but gained 14.8 % less body weight, 21.4 % less WATW, and 17.6 % less BATW than the rats fed the CK diet. This suggests that increased chicken protein in the diet could attenuate high-fat-induced body weight gain and adipogenesis without reducing energy intake in rats, which was also observed in other studies on high-protein diets (Magkos, 2020). However, these findings did not support the theory of high satiating effects of high-protein diets (Halton & Hu, 2004).

During obesity development, excess calories are stored in the body as fat. WAT is the primary organ for fat storage and can be divided into subcutaneous (located underneath the skin) and visceral WAT (around the abdominal organs). As male–female differences may affect body fat distribution (Freedman et al., 1990), only male rats were chosen for this study. Visceral WAT is thought to exert more adverse health effects than subcutaneous WAT (Murphy et al., 2021). In rodents, the epididymal visceral fat pad expands more than other fat depots during the early stages of high-fat diet feeding (Van Beek et al., 2015; Murphy et al., 2021). In the present study, increasing dietary chicken protein reduced lipid accumulation in the epididymal fat pad by 18.4 %, and this reduction extent was quite similar to the reduction extent (by 18.8 %) of the adipocyte size of EAT. These results indicate that decreased EAT expansion was mainly attributed to decreased adipocyte hypertrophy (decrease in size).

Excessive visceral fat and central adiposity are strong risk factors for insulin resistance and type 2 diabetes mellitus. It was assumed that the reduced body weight and epididymal visceral fat mass due to high chicken protein levels might promote insulin sensitivity in rats fed a high-fat diet. In the present study, fasting serum insulin concentration was significantly reduced by high chicken protein levels compared to normal chicken protein levels. This was consistent with our previous studies, which showed that blood insulin concentrations were reduced by normal levels of chicken protein compared with the same level of casein (Song et al., 2016). Blood GSP levels accurately reflect the degree of glycemia over a period of several days to two weeks before measurement (Kennedy, Mehl, Riley, & Merimee, 1981). Blood GSP concentration in the HCK group was significantly lower than that in the CK group. This was consistent with the reduced blood insulin concentration caused by the HCK diet. However, OGTT results and HOMA-IR indices did not differ between the HCK and CK diet groups. Therefore, it could be concluded that, compared to the CK diet, the HCK diet reduced blood insulin and glycemia but had no effect on insulin resistance and blood glucose clearance ability in rats. Interestingly, Vanessa et al. (2002, 2006, 2008) reported that a chicken-based diet reduced albuminuria and improved the serum fatty acid profiles in patients with type 2 diabetes with diabetic nephropathy, suggesting that a diet with chicken as the only source of meat may represent an alternative strategy for the treatment of patients with type 2 diabetes and albuminuria (Gross et al., 2002; de Mello, Zelmanovitz, Perassolo, Azevedo, & Gross, 2006; de Mello, Zelmanovitz, Azevedo, de Paula, & Gross, 2008). However, the molecular mechanisms underlying the effects of dietary chicken proteins on blood insulin regulation remain unclear.

In addition to insulin resistance, obesity is characterized by low-grade systemic inflammation (Heymsfield & Wadden, 2017). Adipocytes are the most important source of leptin and circulating leptin levels are directly correlated with adipose tissue mass (Fantuzzi, 2005). In the current study, although the difference was not significant, intake of high levels of chicken protein reduced blood leptin concentrations in rats by 16.6 %, which is in line with the reduced EATW/FBW (by 18.4 %) and adipocyte area (by 18.8 %). Adipose-resident immune cells and endothelial cells are the main sources of other adipokines, including MCP-1, TNF-α, and IL-6 (Martins, Oliveira, Cruz, Torres-Leal, & Marreiro, 2014). The dysregulated production or secretion of these adipokines causes adipose tissue dysfunction and has been implicated in obesity-induced inflammation and insulin resistance (Martins et al., 2014). In the current study, levels of blood inflammatory factors, including TNF-α, IL-6, IL-1b, and IL-10, did not change. However, blood MCP-1 concentration in rats fed the HCK diet was 38.0 % lower than that in rats fed the CK diet, although the difference did not reach the statistically significant level, indicating a tendency of reduced systemic inflammation by HCK diet.

Adipose tissue plays an essential role in regulating lipid and energy homeostasis (Tchkonia et al., 2013), and obesity is closely related to metabolic disorders of the adipose tissue (Heymsfield & Wadden, 2017). Here, we conducted a transcriptomic analysis of epididymal adipose tissue to identify differentially expressed genes and related metabolic pathways. In accordance with the reduced adipocyte size, the mRNA expression of lipid biosynthetic processes, including the biosynthesis of cholesterol, triglycerides, phospholipids, and fatty acids, was markedly downregulated by the HCK diet. Notably, these gene set groups, especially cholesterol biosynthesis, overlapped with the top 50 downregulated genes in the HCK group, indicating that the mRNA expression of cholesterol biosynthesis was the most downregulated biological process in the adipose tissue of rats fed the HCK diet.

The top down-regulated genes related to lipid metabolism were *Insig1*, *Ptgis*, *Srebf2*, *Angptl4*, *Hmgcs1*, and *Fasn*. Correlation analysis showed that the adipocyte area positively correlated with the mRNA expression of *Insig1* and *Ptgis*. *Insig1* is an important upstream regulator of sterol regulatory element binding protein (SREBP) cleavage activation as it retains the SREBP-SCAP complex in the endoplasmic reticulum (Attie, 2004). Cholesterogenesis and lipogenesis are regulated by insulin through the regulated expression of the SREBPs (Eberlé, Hegarty, Bossard, Ferré, & Foufelle, 2004). In this study, the blood insulin concentrations were significantly reduced by the HCK diet. There are three major SREBP isoforms, namely SREBP-1a, SREBP-1c, and SREBP-2, which are encoded by two genes (Eberlé et al., 2004). The SREBP-2 isoform, encoded by *Srebf2*, predominantly affects cholesterol homeostasis through the regulation of HMG-CoA synthase (*Hmgcs*), and moderately affects genes involved in fatty acid synthesis, such as *Fasn* (Horton et al., 2003). In the current study, correlation analysis showed that the mRNA expression of *Insig1* positively correlated with that of *Srebf2* and *Fasn*. Moreover, the mRNA expression of *Srebf2*, *Hmgcs*, and *Fasn* positively correlated with each other. These findings suggest a potential molecular mechanism for the fat-reducing effects of the HCK diet, which could be that the HCK diet reduced insulin and downregulated the expression of its downstream genes, *Insig1* and *Srebf2*. The downstream genes of *Srebf2* and the expression of *Hmgcs* and *Fasn* participating in cholesterol and fatty acid synthesis were also downregulated.

Additionally, correlation analysis showed that fasting blood insulin and GSP levels positively correlated with the mRNA expression of *Angptl4*, which, in turn, positively correlated with *Ptgis* mRNA expression. Angptl4, which is primarily secreted from adipose tissue, is a critical regulator of TG hydrolysis through the inhibition of lipoprotein lipase activity (Zhang & Zhang, 2022). In the present study, *Angptl4* was downregulated (FC = -2.63) by HCK diet. However, this was unexpected because Angptl4 is a fasting-induced factor that changes in a direction opposite to that of insulin (Kroupa et al., 2012). However, further studies are needed to verify this observation. This study suggests that chicken protein may be a good protein source for weight control. A diet with chicken as the only source of meat may represent an alternative strategy for the treatment of patients with type 2 diabetes. This study could promote the understanding of the health effects of chicken protein.

5. Conclusions

In conclusion, this study investigated the effects of high and normal chicken protein levels on the development of obesity induced by high-fat diets. Compared to normal levels of chicken protein (CK diet), high levels of chicken protein (HCK diet) resulted in a significant reduction in body weight gain (by 15 %), EATW (by 18.4 %), and EAT adipocyte size (by 18.8 %) in rats without affecting food intake. Compared to the CK diet, the HCK diet reduced blood insulin and glycemia but had no effect on insulin resistance or the blood glucose clearance ability in rats. EAT transcriptomics related to lipid biosynthesis, carbohydrate and energy metabolism, protein translation, and the cell cycle were extensively downregulated by the HCK diet. The mRNA expression of cholesterol biosynthesis was the most downregulated biological process in the WAT of rats fed the HCK diet, which could be related to the top down-regulated hub genes, such as *Insig1*, *Srebf2*, *Hmgcs*, and *Fasn*. Further studies are required to elucidate the molecular mechanisms underlying the effects of chicken proteins on insulin and lipid metabolisms.

Funding

This work was supported by the National Natural Science Foundation of China [grant number 32202099], Jiangsu Provincial Department of Education [grant number 21KJB550008], Jiangsu Innovative Group of Meat Nutrition, Health and Biotechnology, Jiangsu Agricultural Industry Technology System [grant number JATS [2021] 024], and the Excellent Scientific and Technological Innovation Team of Colleges and Universities of Jiangsu Province [grant number SUJIAOKE [2021] No.1].

Ethics Statement

All animals were handled in accordance with the guidelines of the Ethical Committee of Experimental Animal Center of China Pharmaceutical University (the license number is SYXK (Su) 2018-0019).

CRediT authorship contribution statement

Shangxin Song: Investigation, Funding acquisition, Writing – original draft. **Yulin Gao:** Investigation. **Tianlan Xia:** Visualization, Validation. **Yefei Zhou:** Data curation, Validation. **Guido J.E.J. Hooiveld:** Methodology, Software. **Michael Muller:** Conceptualization, Methodology. **Chunbao Li:** Supervision, Funding acquisition, Writing – review & editing.

Declaration of Competing Interest

The authors declare that they have no known competing financial interests or personal relationships that could have appeared to influence the work reported in this paper.

Data availability

Data will be made available on request.

Appendix A. Supplementary material

Supplementary data to this article can be found online at https://doi.org/10.1016/j.jff.2023.105713.

References

Attie, A. D. (2004). Insig: A significant integrator of nutrient and hormonal signals. *Journal of Clinical Investigation, 113*(8), 1112–1114. https://doi.org/10.1172/JCI21450

Bourgon, R., Gentleman, R., & Huber, W. (2010). Independent filtering increases detection power for high-throughput experiments. *Proceedings of the National Academy of Sciences of the United States of America, 107*(21), 9546–9551. https://doi.org/10.1073/pnas.0914005107

Carlin, G., Chaumontet, C., Blachier, F., Barbillon, P., Darcel, N., Blais, A., … Davila, A.-M. (2019). Maternal high-protein diet during pregnancy modifies rat offspring body weight and insulin signalling but not macronutrient preference in adulthood. *Nutrients, 11*(1). https://doi.org/10.3390/nu11010096

Cacho, J., Sevillano, J., de Castro, J., Herrera, E., & Ramos, M. P. (2008). Validation of simple indexes to assess insulin sensitivity during pregnancy in Wistar and Sprague-Dawley rats. *American journal of physiology. Endocrinology and metabolism, 295*, E1269–E1276. https://doi.org/10.1152/ajpendo.90207.2008

De Mello, V. D., Zelmanovitz, T., Azevedo, M. J., de Paula, T. P., & Gross, J. L. (2008). Long-term effect of a chicken-based diet versus enalapril on albuminuria in type 2 diabetic patients with microalbuminuria. *Journal of Renal Nutrition, 18*(5), 440–447. https://doi.org/10.1053/j.jrn.2008.04.010

De Mello, V. D., Zelmanovitz, T., Perassolo, M. S., Azevedo, M. J., & Gross, J. L. (2006). Withdrawal of red meat from the usual diet reduces albuminuria and improves serum fatty acid profile in type 2 diabetes patients with macroalbuminuria. *The American Journal of Clinical Nutrition, 83*(5), 1032–1038. https://doi.org/10.1093/ajcn/83.5.1032

Drummen, M., Tischmann, L., Gatta-Cherifi, B., Adam, T., & Westerterp-Plantenga, M. (2018). Dietary Protein and Energy Balance in Relation to Obesity and Co-morbidities. *Frontiers in Endocrinology, 9*. https://doi.org/10.3389/fendo.2018.00443

Eberlé, D., Hegarty, B., Bossard, P., Ferré, P., & Foufelle, F. (2004). SREBP transcription factors: Master regulators of lipid homeostasis. *Biochimie, 86*(11), 839–848. https://doi.org/10.1016/j.biochi.2004.09.018

Fantuzzi, G. (2005). Adipose tissue, adipokines, and inflammation. *J Allergy Clin Immunol, 115* (5), 911-919; quiz 920. https://doi.org/10.1016/j.jaci.2005.02.023.

Freedman, D. S., Jacobsen, S. J., Barboriak, J. J., Sobocinski, K. A., Anderson, A. J., Kissebah, A. H., … Gruchow, H. W. (1990). Body fat distribution and male/female differences in lipids and lipoproteins. *Circulation, 81*(5), 1498–1506. https://doi.org/10.1161/01.CIR.81.5.1498

Gross, J. L., Zelmanovitz, T., Moulin, C. C., De Mello, V., Perassolo, M., Leitao, C., … Azevedo, M. J. (2002). Effect of a chicken-based diet on renal function and lipid profile in patients with type 2 diabetes: A randomized crossover trial. *Diabetes Care, 25*(4), 645–651. https://doi.org/10.2337/diacare.25.4.645

Halton, T. L., & Hu, F. B. (2004). The Effects of High Protein Diets on Thermogenesis, Satiety and Weight Loss: A Critical Review. *Journal of the American College of Nutrition, 23*(5), 373–385. https://doi.org/10.1080/07315724.2004.10719381

Heinrich Böll Stiftung, Friends of the Earth Europe and Bund für Umwelt und Naturschutz (2021). Meat atlas - Facts and figures about the animals we eat. Retrieved from www.friendsoftheearth.eu/meatatlas-2021.

Heymsfield, S. B., & Wadden, T. A. (2017). Mechanisms, Pathophysiology, and Management of Obesity. *The New England Journal of Medicine, 376*(3), 254–266. https://www.nejm.org/doi/10.1056/NEJMra1514009.

Horton, J. D., Shah, N. A., Warrington, J. A., Anderson, N. N., Park, S. W., Brown, M. S., & Goldstein, J. L. (2003). Combined analysis of oligonucleotide microarray data from transgenic and knockout mice identifies direct SREBP target genes. *Proceedings of the National Academy of Sciences, 100*(21), 12027–12032. https://doi.org/10.1073/pnas.1534923100

Iannitti, T., & Palmieri, B. (2010). The obese patient: Clinical effectiveness of a high-protein low-calorie diet and its usefulness in the field of surgery. *Minerva Gastroenterologica e Dietologica, 56*(2 Suppl 1), 1–65.

Kennedy, L., Mehl, T. D., Riley, W. J., & Merimee, T. J. (1981). Non-enzymatically glycosylated serum protein in diabetes mellitus: An index of short-term glycaemia. *Diabetologia, 21*(2). https://doi.org/10.1007/BF00251273

Kroupa, O., Vorrsjö, E., Stienstra, R., Mattijssen, F., Nilsson, S. K., Sukonina, V., … Olivecrona, T. (2012). Linking nutritional regulation of Angptl4, Gpihbp1, and Lmf1 to lipoprotein lipase activity in rodent adipose tissue. *BMC Physiology, 12*(1), 13. https://doi.org/10.1186/1472-6793-12-13

Law, C. W., Chen, Y., Shi, W., & Smyth, G. K. (2014). voom: Precision weights unlock linear model analysis tools for RNA-seq read counts. *Genome Biology, 15*(2), R29. https://doi.org/10.1186/gb-2014-15-2-r29

Liisberg, U., Myrmel, L. S., Fjaere, E., Ronnevik, A. K., Bjelland, S., Fauske, K. R., … Madsen, L. (2016). The protein source determines the potential of high protein diets to attenuate obesity development in C57BL/6J mice. *Adipocyte, 5*(2), 196–211. https://doi.org/10.1080/21623945.2015.1122855

Magkos, F. (2020). The role of dietary protein in obesity. *Reviews in Endocrine & Metabolic Disorders, 21*(3), 329–340. https://doi.org/10.1007/s11154-020-09576-3

Martins, L. M., Oliveira, A. R. S., Cruz, K. J. C., Torres-Leal, F. L., & Marreiro, D. d. N. (2014). Obesity, inflammation, and insulin resistance. *Brazilian Journal of Pharmaceutical Sciences, 50* (4), 677-692. https://doi.org/10.1590/S1984-82502014000400003.

Merico, D., Isserlin, R., Stueker, O., Emili, A., & Bader, G. D. (2010). Enrichment map: A network-based method for gene-set enrichment visualization and interpretation. *PLoS One1, 5*(11), e13984.

Murphy, K. P., Hendley, M. A., Patterson, A. T., Hall, H. E., Carter, G. J., Isely, C., & Gower, R. M. (2021). Modulation of adipocyte size and fat pad weight via resveratrol releasing scaffolds implanted into the epididymal adipose tissue. *Journal of Biomedical Materials Research Part A, 109*(5), 766–778. https://doi.org/10.1002/jbm.a.37063

Ritchie, M. E., Phipson, B., Wu, D., Hu, Y., Law, C. W., Shi, W., & Smyth, G. K. (2015). limma powers differential expression analyses for RNA-sequencing and microarray studies. *Nucleic Acids Research, 43*(7), e47.

Robinson, M. D., & Oshlack, A. (2010). A scaling normalization method for differential expression analysis of RNA-seq data. *Genome Biology, 11*(3), R25. https://doi.org/10.1186/gb-2010-11-3-r25

Robinson, M. D., McCarthy, D. J., & Smyth, G. K. (2010). edgeR: A Bioconductor package for differential expression analysis of digital gene expression data. *Bioinformatics, 26*(1), 139–140. https://doi.org/10.1093/bioinformatics/btp616

Salter, A. M. (2018). The effects of meat consumption on global health. *Revue Scientifique et Technique, 37*(1), 47–55. https://doi.org/10.20506/rst.37.1.2739

Subramanian, A., Tamayo, P., Mootha, V. K., Mukherjee, S., Ebert, B. L., Gillette, M. A., … Mesirov, J. P. (2005). Gene set enrichment analysis: A knowledge-based approach for interpreting genome-wide expression profiles. *Proceedings of the National Academy of Sciences of the United States of America, 102*(43), 15545–15550. https://doi.org/10.1073/pnas.0506580102

Song, S., Hooiveld, G. J., Li, M., Zhao, F., Zhang, W., Xu, X., … Zhou, G. (2016). Distinct physiological, plasma amino acid and liver transcriptome responses to purified dietary beef, chicken, fish, and pork proteins in young rats. *Molecular Nutrition & Food Research, 60*(5), 1199–1205. https://doi.org/10.1002/mnfr.201500789

Song, S., Xia, T., Zhu, C., Xue, J., Fu, Q., Hua, C., … Li, C. (2020). Effects of Casein, Chicken, and Pork Proteins on the Regulation of Body Fat and Blood Inflammatory Factors and Metabolite Patterns Are Largely Dependent on the Protein Level and Less Attributable to the Protein Source. *Journal of Agricultural and Food Chemistry, 68*(35), 9398–9407. https://doi.org/10.1021/acs.jafc.0c03337

Tchkonia, T., Thomou, T., Zhu, Y., Karagiannides, I., Pothoulakis, C., Jensen, M. D., & Kirkland, J. L. (2013). Mechanisms and metabolic implications of regional differences among fat depots. *Cell Metabolism, 17*(5), 644–656. https://doi.org/10.1016/j.cmet.2013.03.008

Van Beek, L., Van Klinken, J. B., Pronk, A. C. M., Van Dam, A. D., Dirven, E., Rensen, P. C. N., … Van Harmelen, V. (2015). The limited storage capacity of gonadal adipose tissue directs the development of metabolic disorders in male C57Bl/6J mice. *Diabetologia, 58*(7), 1601–1609. https://doi.org/10.1007/s00125-015-3594-8

Zhang, R., & Zhang, K. (2022). An updated ANGPTL3-4-8 model as a mechanism of triglyceride partitioning between fat and oxidative tissues. *Progress in Lipid Research, 85*, Article 101140. https://doi.org/10.1016/j.plipres.2021.101140